APPENDIX II.4

PREDICTION OF LINEAR VISCOELASTIC PROPERTIES FOR POLYDISPERSE MIXTURES OF ENTANGLED STAR AND LINEAR POLYMERS: MODIFIED TUBE-BASED MODEL AND COMPARISON WITH EXPERIMENTAL RESULTS

E. van Ruymbeke, R. Keunings, and C. Bailly

4.1 INTRODUCTION

The prediction of linear viscoelasticity (LVE) based on molecular "tube" or "slip-link" models and, very recently, atomistic simulations has received tremendous attention in recent years [1-5]. Major progress has been made, to the point that quite accurate quantitative predictions can now be made for linear polymers [6-9], including inverse predictions of molecular weight distributions from knowledge of rheological response [10, 11]. The situation for branched polymers is much more complicated for at least two reasons. First, because of the incredible variety of architectures that can be, and are actually, made in the lab or by industry. Many more parameters are needed to describe complex branched architectures than linear ones, which can adequately be reduced to a few moments of a molecular weight distribution or a limited number of fractions. Second, it has been recognized quite early that branched polymers are characterised by very broad distributions of relaxation times, which are very dependent on details of the architecture [12]. Linear polymers relax mainly by reptation, whereby they diffuse curvilinearly along their confining tube. Reptation times scale as the third power of molecular weight

(MW). For star polymers [13], as for linear chains, the entanglement network prevents motions of the chain across the tube. But, in this case, branch points also prevent reptation. Stress in star polymers relaxes instead by arm fluctuations: the free end of an arm can retract along its own tube and then explore a new path by extending back in another direction. Retraction is entropically unfavorable and therefore thermally activated. As a consequence, stress relaxation in star polymer melts slows down exponentially with increasing arm lengths. This exponential separation of relaxation times reveals a constraint release mechanism called dynamic dilution [12, 14, 15] where the fast fluctuating parts of the polymer act as solvent for the slowly relaxing ones. To address the issue of branched architectures from a molecular theory standpoint, it is quite essential to study model systems with a limited and controlled level of complexity. This explains why many recent studies [3, 16-19] have been devoted to the prediction of LVE for ideal model molecules, mainly monodisperse stars, H-shaped or POM-POM molecules and combs. Some studies on simple mixtures of star architectures [20] or mixtures of stars with linear chains [21, 22] or asymmetric stars [23] have been published also. For the analysis of more complex structures, two main molecular approaches have been proposed. The first one involves the hierarchical description of an explicitly described complex molecule, leading to a hierarchy of relaxation processes [24-26]. Another approach is to empirically reduce the complex architecture to a mixture of simple model molecules (for instance POM-POM molecules [19, 27]), which will of course also implicitly reflect the hierarchy of the real architecture. Even for simple mixtures of model branched and linear molecules, there is no unified molecular approach at the moment. Each system described in the literature requires its own adapted version of reptation/fluctuations theory. There is a strong need for “unified models”, valid for broader ranges of architectures. The objective of this work is to propose a model suitable for predicting LVE of arbitrary mixtures of stars and linear molecules: monodisperse (a)symmetric star or linear polymers, bidisperse star or linear polymers, mixtures of linear and star molecules and polydisperse linear polymers. The success of this model in describing the relaxation of this already broad range of polymer structures gives some hope for

understanding the dynamics of more complex systems. Of particular interest would be an understanding of the behaviour of sparsely branched polymers. Our objective is to deal with arbitrary mixtures of linear chains and (asymmetric) stars, where the interrelation of relaxation processes cannot be predicted a priori. Therefore, we need to rely on a time-marching algorithm that predicts the relaxation at time t from the relaxation state a short time earlier by including progressively the constraint release solvent coming from the various relaxation processes. In particular, our model does not rely on a time scale separation between reptation and fluctuations processes. This is new in comparison with published models [21-23], which consider the reptation solvent as a step function. We analyse the influence of the polymer solvent on the fluctuations and reptation processes by using a similar approach to the one proposed by Graessley for bidisperse mixtures of linear chains [4, 28], and compare our theory with a large set of experimental data taken from the literature.

4.2 THEORY

In this section, we present a modified tube-based model suitable for the prediction of LVE properties for arbitrary mixtures of entangled linear and symmetric or asymmetric star molecules. While our work relies heavily on the large body of literature devoted to tube theories for linear and star polymers [2,3,21,22,23,28,29], we have modified existing models to adapt them to polydisperse systems where time scales for fluctuations and reptation are not necessarily separated. Specific modifications of existing models have been highlighted. In Section 2.1, the global equation used for the calculation of the relaxation modulus is described and commented upon. Since there is no analytical solution for arbitrary mixtures of molecules, we have to rely on a time-marching algorithm for calculating the relaxation function $F(t)$. This is explained in Section 2.2. In Sections 2.3 to 2.7, we discuss the various contributions to the relaxation: fluctuations, reptation, influence of the environment and their interrelationships. In Section 2.8, we briefly describe the numerical implementation of the model.

4.2.1 Relaxation modulus for complex mixtures of linear and star polymers

When a small strain is imposed on an entangled polymer, chain segments orient along the flow direction. At very short times, the chains still relax as if they were in dilute solution, through Rouse motions. However, very soon, they feel the topological constraints arising from the existence of entanglements. This is modelled by the notion of a tube and a primitive chain, which are essentially a coarse grained representation of the true situation [2]. The tube prevents the (primitive) chain from retracting fully at equilibrium. The equilibrium tube length (L_{eq}) and tube diameter (a) are inversely related and linked to the molecular weight between entanglements (M_e) in the following way:

$$L_{eq} \propto a^{-1} \propto M_e^{-1/2} . \qquad (1)$$

Upon deformation, the tube orients and the primitive chain progressively loses its memory by three relaxation mechanisms: reptation and tube length fluctuations, which relax orientation from the ends of the chain, and constraint release which acts on all segments indifferently. The relative importance and corresponding rates of the various relaxation mechanisms will depend on details of the molecular architecture. Reptation is the main relaxation mechanism for linear chains but is also relevant for asymmetric stars at times when fluctuations of the shorter arms are fast. Tube length fluctuations are the main relaxation mechanism for symmetric stars but also act on linear chains, which can be seen as « two-arm » stars. When the polymer melt is partly relaxed by reptation or fluctuations, only a fraction of the topological constraints remains active and each molecule can be seen as if it were confined in a widened tube limited by the entanglements which are still effective. This is modelled by "tube dilation" or "dynamic dilution" concepts pioneered by Marrucci [14] and Ball-McLeish [12]. At a time when $\Phi(t)$ is the remaining portion of unrelaxed tube segments by reptation or fluctuations, L_{eq}, a and M_e have to be renormalized in the following way :

$$L_{eq}(t) = L_{eq}(0).\left(\Phi(t)\right)^{\alpha/2} \quad , \tag{2}$$

$$a(t) = \frac{a(0)}{\left(\Phi(t)\right)^{\alpha/2}} \quad , \tag{3}$$

$$M_e(t) = \frac{M_e(0)}{\Phi(t)^{\alpha}} \quad . \tag{4}$$

The exponent α is the dilution exponent [29-31]. The complementary fraction *1-Φ(t)* is usually referred to as "the solvent" because it dilutes the entanglement network. The real molecular weight between entanglements does of course not change with time, but the molecular weight between those entanglements that play an active role in the orientation of the molecules does increase with the solvent concentration. This is the well-known picture of a "skinny" real tube in a wider "effective" tube. Tube dilation speeds up reptation and fluctuations but it also relaxes the orientation of internal segments by reducing the number of entanglements. It is thus a constraint release mechanism, which can be modelled either by "tube Rouse motions" or "double reptation" [32, 33] concepts. The latter, although only a "mean field" approximation of the real constraint release mechanism, works well in a wide variety of cases [8] and is easy to implement in numerical or analytical schemes.

The relaxation function *F(t)* calculates the fraction of primitive chain segments still oriented at time *t*. Since we are dealing with linear chains and stars of arbitrary distribution, we first have to consider all types of arms. Linear chains are modelled as two-arm stars. Let φ_i be the volumetric fraction of each type of arm. The location of an arbitrary primitive chain segment along an arm can be represented by the normalised curvilinear variable x_i, ranging from 0 at the end to 1 at the center or branching point. Because tube dilation reduces the length of a complete arm and its tube segments in the same proportion, we do not have to renormalize x_i upon tube dilation. We use the following expression for the relaxation modulus *G(t)*:

$$G(t)=G_N^0 \cdot \left[\sum_i \varphi_i \int_0^1 \left(p_{rept}(x_i,t) \cdot p_{fluc}(x_i,t) \cdot p_{envir}(x_i,t) \right) dx_i \right]. \quad (5)$$

The bracketed expression corresponds to $F(t)$ while G_N^0 is the rubber plateau modulus. Eq. (5) sums up all contributions from segments along all types of arms. A given segment will contribute to the modulus if it has not relaxed by any of the three possible relaxation mechanisms. In this expression p_{rept}, p_{fluct} and p_{envir} represent the probabilities that the segment survives (i.e. remains oriented) by reptation, fluctuations or influence of the environment (constraint release) respectively. We assume the reptation and fluctuations processes to be independent. The constraint release factor in the integral (p_{envir}) represents the probability that a segment is not relaxed by the environment [14, 34]. All three relaxation mechanisms and their interrelations are discussed in detail below.

This formulation for $G(t)$, although different from the one reported by Milner and McLeish [3, 20, 21], describes essentially the same physics. It has the advantage of being well adapted to our problem because it allows for an explicit time dependence of the survival probabilities. This is very important when dealing with reptation as a continuous relaxation process, as opposed to a step function as in [21, 23]. In particular, the expression (5) gives essentially identical results to the one described in [20] for mixtures of monodisperse stars, when applying the same models for calculating relaxation times.

4.2.2 Time-marching algorithm

At any given time, the relaxed fraction of polymer is acting as a solvent for the relaxation of oriented segments, thereby modifying their characteristic reptation and fluctuations times. As the solvent fraction keeps increasing with time, reptation and fluctuations times change continuously. Because of the arbitrary nature of the polymer mixture, there is no way to describe these changes analytically. Therefore we resort to a time-marching algorithm. Along a discretized

time axis, survival probabilities at a given time t_k are calculated from the corresponding values at the previous time t_{k-1}. For a given relaxation mechanism, the survival probability at t_k is the product of the survival probability at t_{k-1} and the survival probability during the Δt interval comprised between t_{k-1} and t_k:

$$p_{fluc}(x_i,t_k) = p_{fluc}(x_i,t_{k-1}) \cdot p_{fluc}(x_i,[t_{k-1},t_k]) \ , \qquad (6)$$

$$p_{rept}(x_i,t_k) = p_{rept}(x_i,t_{k-1}) \cdot p_{rept}(x_i,[t_{k-1},t_k]) \ . \qquad (7)$$

The survival probability during the time interval Δt can be calculated from knowledge of the corresponding relaxation time at t_k, assuming that Δt is small enough to neglect the variation of the relaxation time during the interval:

$$p_{survival}(x_i,[t_{k-1},t_k]) = \exp\frac{-(\Delta t)}{\tau_{relax}(x_i,t_k)} \ . \qquad (8)$$

4.2.3 Relaxation by fluctuations

A. Potential-controlled fluctuations

The equilibrium length of an arm corresponds to the minimum potential energy U resulting from the balance of the arm entropic spring force and of the tube constraint [3]:

$$U(x_i) = \frac{3kT}{2Nb^2}(L_{eq}x_i)^2 + const. \ , \qquad (9)$$

where x_i is position of the end of the arm. This equilibrium length L_{eq} is only the most probable one. The true length fluctuates around the equilibrium value. Any fluctuations shortening the tube will relax the external segments. Ever deeper fluctuations require exponentially increasing times:

$$\tau_{fluc}(x_i) = \tau_0 \ \exp\left(U(x_i)/kT\right) \quad , \quad (10)$$

where τ_0 is a characteristic waiting time. Because the time scale of relaxation by fluctuations increases exponentially with segment depth, external segments will be fully relaxed at times when internal ones remain fully unrelaxed. Consequently, relaxed external segments can be considered as solvent for unrelaxed internal ones. This is the dynamic dilution mechanism described by Ball and McLeish [12]. Because of dynamic dilution, the effective molecular weight between entanglements becomes an increasing function of the fluctuations depth: $M_e(x_i)=M_{e0}/\Phi^{\alpha}(x_i)$, where $\Phi(x_i)$ is the unrelaxed polymer fraction if the fluctuations depth of the arm i is x_i. This leads to the following expression for the relaxation time by fluctuations [35]:

$$\frac{\partial \ln \tau(x_i)}{\partial x_i} = 3 \cdot \left(\frac{M_i}{M_{e0}}\right) \cdot x_i \cdot \Phi(x_i)^{\alpha} \quad . \quad (11)$$

B. Early fluctuations

As long as tube length fluctuations of an arm remain unconstrained by the tube ($U(x) < kT$), the arm end does not feel the potential, nor does it feel the influence of the branching point. The motion of the arm end occurs therefore by an unconstrained Rouse process, with the time to relax up to a fractional distance x proportional to the fourth power of x [2, 3]:

$$\tau_{early}(x_i) = \frac{9\pi^3}{16} \cdot \left(\frac{M_a}{M_{e,0}}\right)^2 \cdot \tau_{R,chain} \cdot x_i^{\,4} . \quad (12)$$

In this expression, $\tau_{R,chain}$ is the Rouse time of the arm and M_a the molecular weight of the arm. The expression (12) can be rewritten as a function of the absolute distance $s = x.L_{eq}$ from the chain-end :

$$\tau_{early}(s) = \frac{9\pi^3}{16} \cdot \left(\frac{M_a}{M_e} \right)^2 \cdot K_{Rouse} \cdot M_a{}^2 \cdot \left(\frac{m_0{}^2 \cdot s^4}{b^4 \cdot M_a{}^4} \cdot M_e{}^2 \right) = \frac{9\pi^3 m_0{}^2 K_{Rouse}}{16 b^4} \cdot s^4, \tag{13}$$

with b the monomer equivalent length and m_0 the monomer molecular weight. It can be seen that the distance s travelled by the arm end does not depend on the arm length, nor on tube width, as expected.

C. Transition between early fluctuations and fluctuations in the potential

From Eqs. (10) and (11), the fluctuations depth corresponding to a potential level equal to kT is easily determined. We call it x_{trans}. The relaxation of segments closer to the arm end will occur by the unconstrained Rouse process while deeper segments will fluctuate in the potential after a waiting time equal to $\tau_{early}(x_{trans,i})$:

$$\tau_{fluc}(x_i) = \tau_{early}(x_i) \qquad for \;\; x_i < x_{trans,i}, \tag{14}$$

$$\tau_{fluc}(x_i) = \tau_{early}(x_i) \exp\left(\frac{\Delta U(x_{trans,i} \rightarrow x_i)}{kT} \right) \;\; for \;\; x_i > x_{trans,i} \; . \tag{15}$$

In this way, the fluctuations time for any depth x is determined and can be used in the expression for the survival probability by fluctuations (8). This method differs from the one proposed by Milner and McLeish [3], which requires the explicit calculation of the waiting time. This becomes very cumbersome for complex mixtures of stars and linear chains and requires an ad hoc cross-over function for the transition between early fluctuations and fluctuations in the potential. In the case of monodisperse stars, the two methods give very similar results.

D. Relaxation by fluctuations for mixtures of symmetric stars

Here, we use the theory developed by Blottière et al. [20] without modification. For a mixture of stars of different arm lengths, the

transition segments between relaxed and unrelaxed portions of the tube are all linked by the equality of their potential. This leads to the following expression:

$$x_2 = \sqrt{\frac{M_1}{M_2}} \cdot x_1 , \qquad (16)$$

where x_1 and x_2 are the corresponding transition segments on chains of arm lengths M_1 and M_2 respectively. From this expression, the overall unrelaxed fraction $\Phi(x)$ can be easily calculated and used in Eq. (11).

4.2.4 Relaxation by reptation

A. Reptation of linear chains

The probability that a given segment of a linear chain relaxes by reptation has been determined by Doi and Edwards [2]:

$$p(x_i, t) = \sum_{p\ odd} \frac{4}{p\pi} \sin\left(\frac{p\pi x_i}{2}\right) \exp\left(\frac{-p^2 t}{\tau_{rept}}\right) , \qquad (17)$$

where τ_{rept} is the reptation time of the chain and x is the normalized position along the chain. The reptation time scales like the cube of the molecular weight:

$$\tau_{rept}(M) = 3\ \tau_e \left(\frac{M}{M_e}\right)^3 = \frac{\zeta\ N_e^2 b^2}{\pi^2 kT} \left(\frac{M}{M_e}\right)^3 , \qquad (18)$$

where τ_e is the Rouse time of a segment, ζ is the monomeric friction coefficient, and N_e is the number of monomers in a segment. As the polymer relaxes by reptation, its equilibrium length shrinks and the tube widens (Eq.(2) and (3)). This will have an impact on τ_{rept}, which

should scale as $\Phi^{\alpha}(t)$ [34]. However, even if the molecule has the time to explore the widened tube at the time scale of τ_{rept}, the effect of dynamic dilution is not necessarily felt by the reptation process. For instance, Graessley [28] has shown that, in a bidisperse mixture of short and long entangled molecules, the long molecules will reptate in the tube widened by the fast relaxation of the short molecules (as opposed to the skinny tube) only if their reptation time is long with respect to their constraint release Rouse time:

$$Gr = \frac{\tau_{rept}(M_2)}{\tau_{CR\ Rouse}(M_2)} = \frac{KM_2^3}{KM_1^3 \cdot Z_2^2} > 1, \qquad (19)$$

where M_1 and M_2 are the molecular weights of the short and long chains, respectively, and Z_2 is the number of segments of the long chains. Park and Larson have used this concept very recently in [4]. The non-dimensional ratio $\tau_{rept}/\tau_{CR,\ Rouse}$ is called the Graessley number. This criterion is easily understood in the following way: the tube can be dilated by the slow removal of entanglements but reptation in the dilated tube requires correlated release of entanglement constraints and can only occur if constraint release is fast w.r.t. the reptation time of the test chain. (see Figure 1).

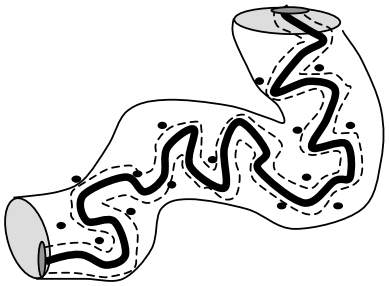

Figure 1: If the constraints(•) are released at the same time scale as the reptation time of the chain, the latter occupies the skinny dashed tube. If the constraints move fast w.r.t. the reptation time of the chain, the latter can occupy the wider continuous tube.

Some experimental studies have partially confirmed this rule [36, 37], in the sense that a ratio of 0.1 instead of 1 has to be used. It is clearly not sufficient for a fraction of the polymer to be relaxed by reptation to be automatically considered as solvent for the reptation process of the longer molecules. In most cases, the required separation of time scales is not obeyed, or only obeyed for a small fraction of the chains in typical polydisperse distributions. In that case, we have to consider that reptation occurs in the skinny tube rather than the wider effective tube. There is no criterion equivalent to the Graessley number for the solvent coming from fluctuations. In this paper, we will test the various possible options of including or excluding the solvent coming from fluctuations or reptation for the calculation of the reptation time. In general, we can write [34]:

$$\tau_{rept}(t) = \tau_{rept,0}\ \Phi^{\alpha}_{active}(t), \qquad (20)$$

where τ_{rept0} is the reptation time at time 0 and $1-\Phi_{active}(t)$ is the solvent fraction that has appeared long enough before time t to be included in the reptation solvent ($1 \geq \Phi_{active}(t) \geq \Phi(t)$).

Most papers [13, 22] consider that a linear chain is relaxed by reptation when its center of mass has diffused a distance $L_{eq0}.\ (1-x_{rel\text{-}fluct})$ along the tube, where $x_{rel\text{-}fluct}$ is the fractional distance of the deepest segment relaxed by fluctuations at that time. This implies that the external segments relaxed by fluctuations no longer play a role in the reptation process. As explained before, we prefer to consider that the diffusion of the center of mass has to occur on a distance equal to the length of the effective tube, i.e. $L_{equ0} / \Phi_{active}^{0.5\alpha}$ as proposed by Marrucci and Viovy[14, 34].

B. Reptation of asymmetric stars

An asymmetric star is defined as a three-arm star consisting of two long arms and a short one. Although experimental validations are

limited so far to systems where the two long arms are identical, the same model can in principle be applied to long arms of unequal length, provided that the short arm is indeed the shortest of the three. The two longer arms form the backbone. At times when the short arm can rapidly fluctuate all the way down to the branch point, it will act as solvent for the reptation of the backbone and at the same time as a strong friction point. We use a similar treatment to the one proposed by Frishknecht et al. [23]. The equivalent friction coefficient of the small arm is naturally defined as:

$$\frac{\zeta_{arm}}{kT} = \frac{\pi^2 \tau_{fluc,small\ arm}}{a^2}, \tag{21}$$

where $\tau_{fluc\ small\ arm}$ is the fluctuations time of the short arm to the branch point, and a is the equilibrium length between two entanglements. The total friction coefficient of the reptating backbone is the combined friction coefficient coming from the fluctuating arm (often the dominating part) and of the ordinary linear segments:

$$\zeta_{tot} = \zeta_{lin} + \zeta_{arm}, \tag{22}$$

$$\frac{\zeta_{lin}}{kT} = \frac{\pi^2 \tau_e}{a^2} \cdot Z, \tag{23}$$

where τ_e is the segmental Rouse time and Z is the number of linear segments on the backbone. The reptation time of the backbone in the skinny tube is easily calculated from these expressions [23]:

$$\tau_{rept,0}(M_l) = 3 \cdot Z^3 \cdot \tau_e \cdot \left(1 + \frac{\tau_{fluc,small\ arm}}{Z \cdot \tau_e}\right), \tag{24}$$

where M_l is the molecular weight of the backbone. The influence of tube dilation on the reptation time of the backbone is expressed by the same equation as for ordinary linear chains (Eq. (20)). However, there

is no criterion equivalent to the Graessley number [28] for deciding which part of the relaxed polymer fraction has to be considered. We can assume that the solvent coming from fluctuations of the short arm and from fluctuations of the long arms up to the length of the short arm must be taken into account for the backbone reptation, since the latter only occurs at much longer times than $\tau_{fluc,\ small\ arm}$. On the other hand, the reptation solvent coming from the external segments of the backbone will not influence the backbone reptation time (no time separation). Deeper fluctuations of the long arms will be included or not depending on the time scale separation of the processes. As the fluctuations times of the arms and the reptation time of the backbone are interrelated in a complex way, a time-marching algorithm is essential if we want to consider the reptation process as continuous (as opposed to a step function).

The expression used for τ_{rept} in this work (Eq. (24)) is very similar to the one used by Frishknecht et al. [23] with a significant difference. We do not allow the equivalent friction coefficient of the branch point (Eq. (21)) to depend on the architecture of the star molecule (variable parameter p in [23] depending on the molecular weight of the short arm).

4.2.5 Influence of the reptation solvent on fluctuations times

When linear chains are mixed with stars or when asymmetric stars are present, fluctuations are influenced by the solvent coming from reptation as well as the fluctuations solvent. Because the fluctuations potentials of stars with different arm lengths are interrelated (Eq.(16)), fluctuations relaxation times for mixtures of stars only depend on x, rendering the time-dependence implicit. If arbitrary time-dependent reptation solvent is added, the fluctuations times will now explicitly depend on t as well as on x. In this case, a time-marching algorithm is essential. At each time step, the reptation solvent must be updated. It is considered constant during any particular time step, which allows one to calculate the x dependence of the fluctuations times for the arms. First, the reptation relaxation probability is calculated for each

segment by Eq(7,17,20). The reptation time is calculated from Eq. (24) in the case of asymmetric stars (see below). This allows one to calculate the global fraction of the polymer still oriented from reptation at time t: $\Phi_{rept}(t)$. The corresponding solvent fraction speeds up fluctuations. Therefore, fluctuations processes originating at time t take place in a widened and shrunk tube according to Eq. (2-4).

The expression for τ_{early} (unconstrained Rouse fluctuations at the end of the arm, with $U< kT$) accounts for the reptation solvent as follows:

$$\tau_{early}(x_i) = \frac{9\pi^3}{16} \cdot \left(\frac{M_a \cdot \phi_{rept}^{\alpha}}{M_{e,0}} \right)^2 \cdot \tau_{R,chain} \cdot x_i^4 . \qquad (25)$$

In this way, the absolute distance s traveled by the arm end in the absence of the fluctuations potential remains independent of the tube dimensions, as it should. However, since $x=s/L_{eq}$, a reduction of L_{eq} arising from tube dilation will result in an increase of the corresponding x value.

For fluctuations in the potential ($U>kT$), the reptation solvent is combined with the fluctuations solvent:

$$\frac{\partial \ln \tau(x_i)}{\partial x_i} = 3 \cdot \left(\frac{M_i}{M_{e0}} \right) \cdot x_i \cdot \Phi_{active}(x_i, t)^{\alpha} , \qquad (26)$$

where $\Phi_{\text{active}}(x_i,t)$ is the "active" unrelaxed fraction, defined as above, and calculated for a given test chain of arm molecular weight M_i relaxed up to x_i by fluctuations. We first calculate the global survival fraction $\Phi(x_i,t)$. Corresponding transition segments for chains of different arm lengths are obtained by the potential equality expression (16). Only segments between these transition segments and the branching points contribute to the value $\Phi(x_i,t)$, except those which are relaxed by reptation at time t (see Eq. (7)).

While separation of fluctuations relaxation times is of course verified for segments along an arm, the time interval separating the moment when the reptation solvent appears and the fluctuations time of a given segment may not be sufficient to satisfy the required time separation for this solvent to be integrated in the fluctuations process. If the separation is satisfied, $\Phi_{active}\ (x_i,t)$ equals $\Phi(x_i,t)$, otherwise, the reptation solvent must not be considered and $\Phi_{active}\ (x_i,t)$ is larger than $\Phi(x_i,t)$. To our knowledge, there is no criterion allowing us to establish which option to take. We have systematically compared the experimental results with the predictions obtained under the two assumptions.

4.2.6 Relaxation by the environment

Besides relaxation by reptation and fluctuations, accelerated or not by tube dilation, a global constraint release mechanism must be considered. We call it « relaxation by the environment ». We use a generalization of double reptation ideas [32, 33] to systems where reptation is not necessarily the dominating relaxation mechanism.

We can consider an average survival probability of oriented segments in the melt. This probability then represents the contribution of the environment to the survival probability of a test segment in the way expressed by Eq. (5). If p_{envir} is properly calculated, the expression (5) will reduce to well known relationships for linear chains under (generalized) double reptation or for symmetric stars under dynamic dilution.

The probability p_{envir} is a conditional survival probability by constraint release of a test segment that has not been relaxed by reptation nor by fluctuations. As this constraint release mechanism is a global one and affects all segments in the same way, the survival probability by the environment is equal to the probability that an entanglement taken at random is still oriented. In effect, it is a “mean field” influence. To calculate this probability, the overall fraction of segments surviving by reptation and fluctuations must be computed. Since the test segment is not relaxed by fluctuations, all segments closer to the centre or the branch point of the test chain and equivalent segments on other chains (i.e. with identical fluctuations potential) are also unrelaxed by

fluctuations but can still relax by reptation. On the other hand, segments closer to the chain-ends can relax by both reptation or fluctuations. This leads to the following expression for p_{envir}, where $x_{k,trans}$ is the fractional distance of segments equivalent (potential-wise) to the test segment x_i:

$$p_{envir}(x_i,t) = \left(\sum_k \varphi_k \cdot \left[\int_0^{x_{k,trans}} p_{rept}(x_k,t)\; p_{fluc}(x_k,t)\; dx_k + \int_{x_{k,trans}}^{1} p_{rept}(x_k,t)\; dx_k \right] \right)^{\alpha}. \tag{27}$$

4.2.7 Constraint release Rouse regime: notion of supertube

Usually, at time t, the global unrelaxed polymer fraction $\Phi(t)$ confining a chain in its effective tube is equal to the proportion of the polymer which is not relaxed by reptation or fluctuations, and can be calculated in our model by the following equation:

$$\Phi(t) = \sum_i \varphi_i \int_0^1 p_{rept}(x_i,t) p_{fluc}(x_i,t) dx_i \tag{28}$$

This leads to a prediction for the effective tube diameter through Eq. (3). But, in some cases, the self-accelerating nature of tube dilation can result in the effective tube widening faster than the chain is able to explore it. Exploration of the tube is limited by the unconstrained Rouse process of the disentangled chain. This imposes a lower bound on the unrelaxed fraction $\Phi(t_i)$ as proposed by Milner and McLeish [21, 29]:

$$\Phi(t_i) \geq \Phi(t_{i-1}) \cdot \sqrt{\frac{\Delta t}{t_i}}. \tag{29}$$

The limitation expressed by Eq. (29) is called the « constraint release Rouse regime » (CRRR). In this situation, the solvent fraction generated by constraint release increases more slowly than the total fraction of segments relaxed by reptation or fluctuations.

4.2.8 Numerical implementation

The model has been implemented in MatLab® in order to predict the relaxation function *G(t)*. The function *G(t)* is in turn inverted to obtain dynamic moduli *G'* and *G"* by use of the well known Schwarzl relations [38]. This approximated method has been preferred over the Fourier Transform approach for its simplicity and associated computational speed. It provides excellent results in the frequency range of the experimental data, except perhaps at the lowest frequencies because of the well known series truncation issue[8, 38].

4.3 EXPERIMENTAL DATA

The data for all the samples analysed in this paper have been taken from the literature or obtained from external sources. We have tested our model on polybutadiene (PBD), polyisoprene (PI) and polystyrene (PS) samples with various architectures (linear, symmetric stars and asymmetric stars). Some samples are mixtures of monodisperse linear or star polymers. The data for the tested PBD, PI and PS samples are summarised in Table 1, 2 and 3.

Table 1: PBD samples

Sample	Nb of arms	Monodisperse or mixture	MW arm (g/mol) or mixture composition	Master curve (°C)	Paper reference
PBD1	4	monodisperse	11300	27	39
PBD2	4	monodisperse	30250	27	39
PBD3	4	monodisperse	40500	27	39
PBD4	2	monodisperse	20700 (total M_W)	28	40
PBD5	2	monodisperse	44100 (total M_W)	28	40
PBD6	2	monodisperse	97000 (total M_W)	28	40
PBD7	2	monodisperse	201000 (total M_W)	28	40
PBD8	3	monodisperse	42330	25	41
PBD9	2	monodisperse	100000 (total M_W)	25	41
PBD10		mixture	20% PBD8, 80% PBD9	25	41
PBD11		mixture	50% PBD8, 50% PBD9	25	41
PBD12		mixture	75% PBD8, 25% PBD9	25	41

Table 2: PI samples

Sample	Nb of arms	Monodisperse or mixture	MW arm (g/mol) or mixture composition	Master curve (°C)	Paper reference
PI1	3	monodisperse	28000	25	20
PI2	3	monodisperse	144000	25	20
PI3		mixture	20% PI1, 80% PI2	25	20
PI4		mixture	50% PI1, 50% PI2	25	20
PI5		mixture	80% PI1, 20% PI2	25	20
PI6	3	monodisperse	104000	25	23
PI7	2	monodisperse	212000 (total M_W)	25	23

PI8	3	asymmetric	107000-107000-11500	25	23
PI9	3	asymmetric	116000-116000-19000	25	23
PI10	3	asymmetric	107000-107000-39000	25	23
PI11	3	asymmetric	113500-113500-38000	25	23

Table 3 : PS samples

Sample	Nb of arms	Monodisperse or mixture	Mw (g/mol) Or mixture composition	Master curve (°C)	Paper reference
PS1	2	monodisperse	355500	170	8
PS2	2	monodisperse	191300	170	8
PS3	2	monodisperse	886900	170	8
PS4	2	monodisperse	176700	170	8
PS5	2	monodisperse	60400	170	42
PS6	2	monodisperse	58400	170	8
PS7	2	monodisperse	676000	170	42
PS8	2	monodisperse	50% PS2, 50% PS3	170	8
PS9	2	monodisperse	35% PS2, 65% PS7	170	8
PS10	2	mixture	65% PS2, 35%PS7	170	8
PS11	2	mixture	80% PS2, 20% PS6	170	8
PS12	2	mixture	20% PS4, 80% PS5	170	42
PS13	2	mixture	80% PS4, 20% PS5	170	42

4.4 RESULTS AND DISCUSSIONS

The model has been validated on a series of experimental data relative to various model systems described in the literature. The model predictions do not include the high frequency Rouse relaxation (unconstrained modes in the tube). This explains why the model does not predict the high frequency upturn of the dynamic moduli.

4.4.1 Polybutadiene (PBD) samples : monodisperse stars and linear chains

We first test our model on narrow disperse linear and star PBD samples. They are indeed the simplest to treat. Experimental results on four-arm stars (PBD1 to PBD3) come from Roovers [39] while the linear polymer samples (PBD4 to PBD7) have been tested by Baumgaertel et al. [40].
The experimental results and model predictions are presented in Figs. 2 and 3.

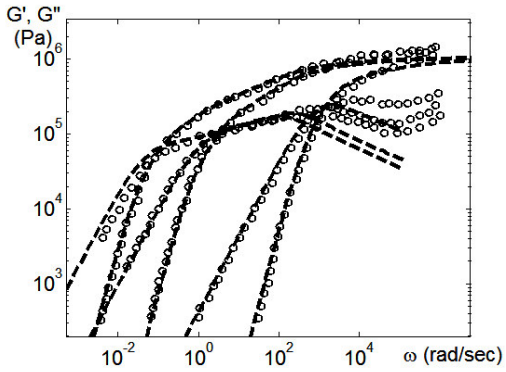

Figure 2: Comparison between predictions of relaxation moduli (dashed lines) and experimental data (unfilled symbols)) for relaxation moduli of four-arm monodisperse stars (from right to left: PBD1, PBD2 and PBD3)

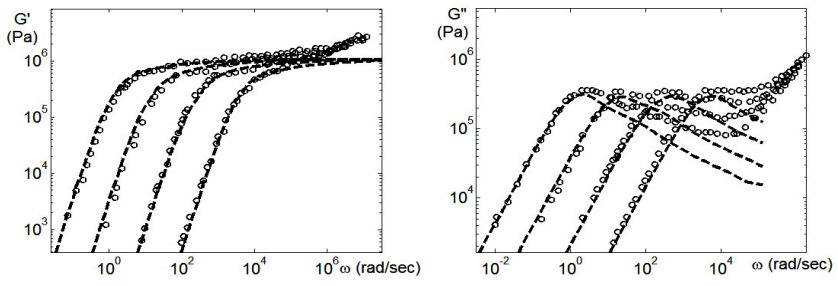

Figure 3: Comparison between predictions (dashed lines) and experimental data (unfilled symbols) for relaxation moduli of linear monodisperses polymers (from right to left: PBD4, PBD5, PBD6 and PBD7)

The model parameters have been fitted on two monodisperse stars (PBD1 and PBD3), to determine M_e, τ_e and G_N^0. In this case, we needed to use a single linear sample PBD4, to determine K_{rept} (with $\tau_{rept} = K_{rept} .M^3$). We have to take a value of K_{rept} three times smaller than the one calculated from τ_e (see Eq. 18). There is no explanation to this discrepancy at this stage. Interestingly, for PI and PS samples (Sections 4.2, 4.4 and 4.5) the theoretical relation between τ_e and K_{rept} can be used. The best fit values are 1.05 MPa for G_N^0, 1650 g/mol for M_e, 7 10^{-7}s for τ_e, and 1.5 10^{-16}s.mol^3.g^{-3} for K_{rept}, to be compared with G_N^0 = 1.15 MPa, M_e = 1550 g/mol et τ_e = 5.6 10^{-7} s proposed by Fetters et al. [4, 43], and Ferry [44]. A dilution exponent of 1.2 has been found to give the best results. These parameters values have been used for all other PBD samples presented in this paper. The predictions in Figures 2 and 3 are excellent. The predicted results concern samples PBD2, an intermediate molecular weight star sample, and PBD 5 to 7, linear PBD samples of increasing molecular weights. The predictions show that the scaling behaviour of our model is correct for linear *and* star polymers (within the tested molecular weight ranges).

4.4.2 Poly-isoprene (PI) samples: mixtures of monodisperse stars

Figure 4 compares experimental results by Blottière et al. [20] and our model predictions for mixtures of two monodisperse PI 3 arm star samples (arm molar mass 28000 and 144000 g/mol.) in various proportions (samples PI1 to PI5).

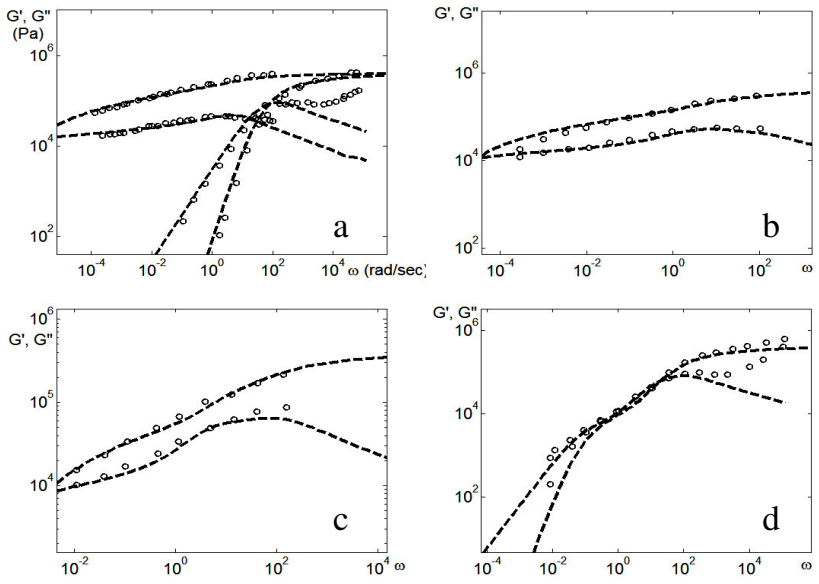

Figure 4: Comparison between predictions (dashed lines) and experimental data (unfilled symbols) for relaxation moduli of two monodisperse stars, PI1 and P12 (a), and their mixtures in different proportions: PI3 (b), PI4 (c), PI5(d).

Model parameters have been fitted on samples PI1 and PI2 [45]. The best fit values are G_N^0 =0.4 MPa, M_e = 3900 g/mol, and τ_e= 8 10^{-6} s. Those values compare well with G_N^0 =0.4 MPa, and τ_e = 8.4 10^{-6} s proposed by Fetters et al [43] and Ferry [44]. Exceptionally, a dilution exponent of 1 is used instead of 1.2, as used by Blottière et al. [20].

The predictions for the mixtures are very good. For mixtures of monodisperse stars, our model essentially reduces to that proposed by Milner and McLeish [3, 20] with however a significant difference concerning the transition between early fluctuations and fluctuations times, as explained in Section 2.3.3. Therefore, the good agreement for mixtures of stars is in fact mainly a test for our treatment of early fluctuations.

4.4.3 PBD samples: mixtures of monodisperse stars and linear molecules

Figure 5 compares experimental results obtained by Struglinski et al. [41] on a 50/50 w/w mixture of a three arm star (arm MW= 42300 g/mol.) and a linear PBD (MW=100000 g/mol) with the predictions obtained by our model without any adjustment of the material parameters obtained earlier. The results for the corresponding pure linear and star polymers are also presented in Fig. 5. The model includes the entire reptation solvent for the calculation of the fluctuations times.

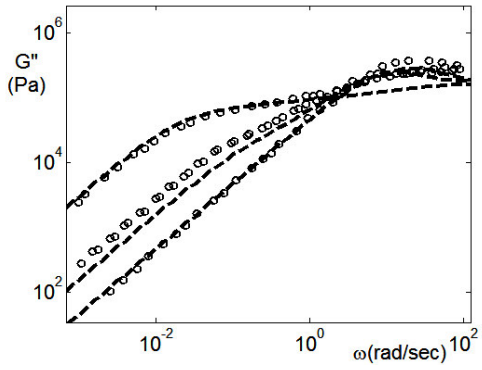

Figure 5: Comparison between predictions (dashed lines) and experimental data (unfilled symbols) for storage modulus of a monodisperse star polymer (PBD8, left curve), a monodisperse linear polymer (PBD9, right curve), and their 50/50 w/w mixture (PBD11, middle curve)

While the predictions are excellent (without any adjustment of parameter values) for the reference monodisperse samples, the model obviously predicts too fast a relaxation of the stars in the case of the mixture, once the linear chains are relaxed (below 1 rad/s). Similar results have been obtained for other mixtures. Since the predictions obtained by the Milner-McLeish model [21] for this type of samples are excellent, it is interesting to understand where the difference comes from. Figures 6a and 6b compare, in log-log and semi-log scales respectively, the global surviving fraction for the 50/50 mixture with or without consideration of the CRRR limitation.

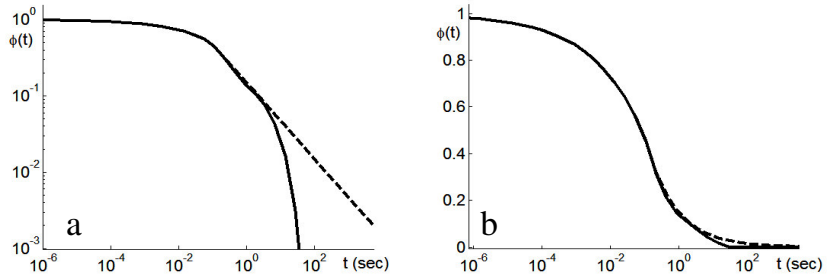

Figure 6: Comparison between the global surviving fraction as function of time for PBD11 with (dashed line) or without (continuous line) consideration of the CRRR limitation, in log-log (6.a) and semi-log (6.b) scale. Reptation solvent is included as a continuous relaxation process.

Indeed, the fraction relaxed by constraint release cannot decrease faster than allowed by the unconstrained Rouse process (Eq. (29)). In Figure 6, we observe that the reptation of the linear chains is slow enough for the stars to have the time to explore their dilated tube below one second. The CRRR only appears later, i.e. at the end of the relaxation process of the stars and has very little influence on the global relaxation, as clearly seen in the semi-log plot (and as opposed to the log-log plot where the CRRR is artificially emphasized). In particular, we have tested the two options presented in Figure 6 and

found very little difference between the predictions of dynamic moduli.

Milner et al. [21] consider reptation as a step function, for the same mixtures of linear and star polymers. This generates a large discontinuity of the global surviving fraction at the time of the reptation of the linear chains and has the effect of magnifying the influence of the CRRR immediately after τ_{rept} and up to a time of $4\tau_{rept}$ for the 50/50 mixture ($\Phi(t_i)$ =0.5 after reptation and $\Phi(t_{i-1})$=1 before reptation in Eq. (29)). This effect is clearly shown in Figure 7.

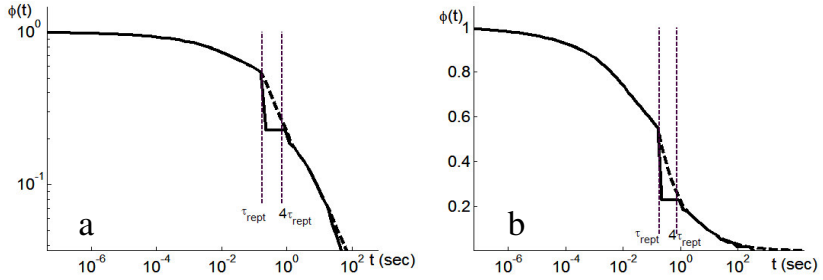

Figure 7: Comparison between the global surviving fraction as function of time (s) for PBD11 with (dashed line) or without (continuous line) consideration of the CRRR limitation, in log-log (7.a) and semi-log (7.b) scale. Reptation solvent is included as a step function relaxation.

Fluctuations times are entirely determined in our model by the progressive increase of the reptation and fluctuations solvent. Since stars are predicted to relax too fast, it seems that the reptation solvent has less of an influence on the fluctuations times in reality than predicted by our model. Are we sure that the stars can entirely use the reptation solvent for their relaxation? In their paper, Milner et al. [21] state that "*the largest tube diameter explored by a chain on time scale τ and the largest tube diameter in which the chain can create unentangled loops on time scale τ do not yield the same answer when*

the tube is dilating". Indeed, a similar reasoning as the one followed by Graessley for mixtures of linear chains [28] can be made in this case. For an arm segment to take advantage of the widened effective tube, its constraint release characteristic time resulting from the reptation of the linear chains has to be smaller than its fluctuations time. Figure 8 illustrates this point.

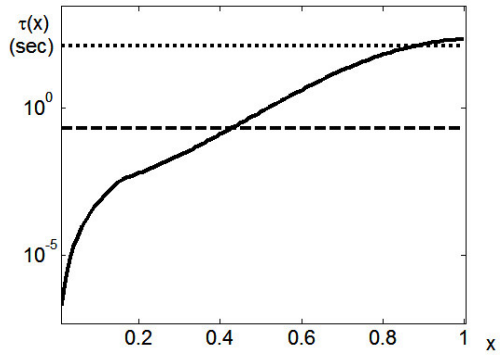

Figure 8: Comparison between the reptation time of linear chains (dashed line), the constraint release characteristic time of the star arms (dotted line), and the fluctuations times of the star arms (continuous line).

The dashed line corresponds to τ_{rept} of the linear chains, the dotted line to the characteristic constraint release time of the star arms, i.e. τ_{rept} $.Z_{arm}^2$, where Z_{arm} is the number of entanglements of the arms, and the continuous line, the fluctuations times of segments along the arms, according to their fractional distance x to the branch point, excluding the reptation solvent. Obviously, reptation of the linear chains and fluctuations of the arms are essentially simultaneous processes in the analyzed mixture, not widely separated ones, and only the deepest segments ($x > 0.9$) can really take advantage of the reptation solvent. The suggestion is that, for this system at least, the reptation solvent influence on fluctuations times should not be considered. Figure 9 compares the experimental results presented by Struglinski et al. [41] for all the tested mixtures with the predictions from our model when

the reptation solvent influence on fluctuations is excluded. The agreement is excellent, which confirms that the stars can apparently not take advantage of the reptation solvent in the fluctuations process, even if they have had the time to explore the dilated tube. In cases where the time scales for reptation and fluctuations are better separated, inclusion of the reptation solvent should work better. Of course, full inclusion or complete exclusion of the reptation solvent are extremes and it would be useful to develop a method allowing progressive inclusion of the reptation solvent.

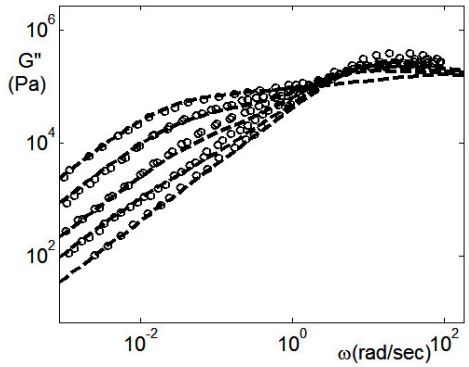

Figure 9: Comparison between predictions (dashed lines) and experimental data (unfilled symbols) for the storage modulus of a monodisperse star polymer (PBD8, left curve), a monodisperse linear polymer (PBD9, right curve), and mixtures in different proportions (PBD10 to PBD12, from right to left). The reptation solvent is excluded for the calculations of the fluctuations times.

4.4.4 PI asymmetric stars

In their paper, Frishknecht et al.[23] study the relaxation of PI asymmetric three arm stars (PI8 to PI11) as well as reference monodisperse linear (PI7, M_w = 212000 g/mol)) and symmetric star (PI6, $M_{w,arm}$ = 104 000 g/mol) samples useful to fit the model parameters. The four asymmetric star samples have all approximately

the same backbone M_w (210 000 g/mol) and short arms ranging from 11 000 g/mol (PI8) to 40 000 g/mol (PI11). We first fit the model on the monodisperse linear and symmetric star samples. We find 1.7 10^{-5} sec. for $\tau_{e,}$, 0.49 MPa pour G_N^0, and 4260 g/mol for M_e (K_{rept} is obtained from $\tau_{e,}$ and M_e [2]). These parameter values are comparable with those obtained by Frishknecht et al. [23] (0.89 10^{-5} sec. for $\tau_{e,}$, 490 MPa pour G_N^0, and 4550 g/mol for M_e), and also relatively close to the ones used for the other series of PI samples analyzed in this paper (Section 4.2). We use a dilution exponent of 1.2 as for all other samples (except for the first series PI samples).

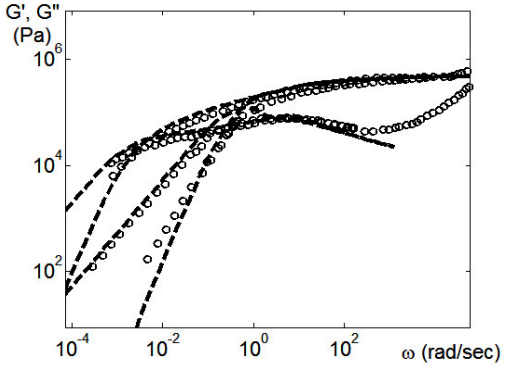

Figure 10: Comparison between fitted (dashed lines) and experimental data (unfilled symbols) for relaxation moduli of a monodisperse PI star (PI6, left curve) and a linear monodisperse PI (PI7, right curve)

Figure 11 presents the comparison between experimental results and predictions from our model for samples PI8 and PI11, using the material parameters reported above. We first consider the assumption that the solvent at time *t* is entirely effective to accelerate the relaxation processes. As Frishknecht et al [23], and despite the fact that we use a slightly different and more favourable expression for the reptation time of the backbone (see Section 2.4.1., last paragraph), we underpredict the backbone reptation time of PI8 while the prediction for PI11 is much better without any adjustment.

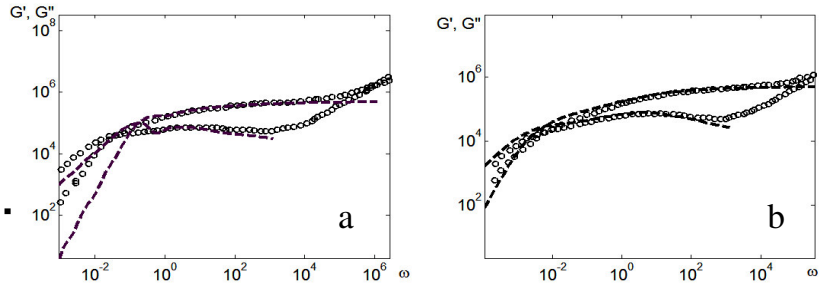

Figure 11: Comparison between predictions (dashed lines) and experimental data (unfilled symbols) for asymmetric star PI8 (a) and asymmetric star PI11 (b). The fluctuations solvent is included in the reptation process.

The origin of the observed discrepancy is the fact that the relaxation process of PI8 cannot fully integrate the backbone fluctuations solvent. Indeed, in Figure 12, we compare the initial backbone reptation time (dotted line) with the fluctuations times of the short arm segments (continuous line) and of the long arms segments (dashed line) for samples PI8 and PI11.

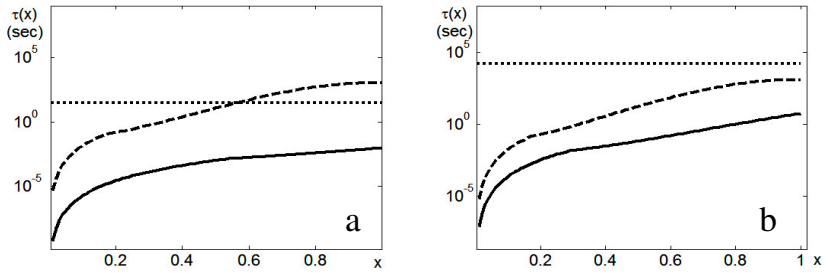

Figure 12: Comparison between the initial reptation time of the backbone (dotted lines), fluctuations times of the short arm (dashed line) and fluctuations times of the long arms (continuous line), for asymmetric star PI8 (a) and asymmetric star PI11 (b).

It is clear that the time scales for reptation of the backbone and for fluctuations of the short arms are separated in all cases. The constraint release of the backbone by fluctuations of the short arm is also time-separated from the reptation of the backbone. This is a consequence of the definition of the reptation of the backbone (see Eq. 24). Therefore, the fluctuations solvent of the short arms must be included when calculating the reptation time of the backbone. On the other hand, fluctuations of the long arms are not time-separated from reptation of the backbone in the case of PI8, and only partially separated in the case of PI11. The constraint release times of the backbone by fluctuations of the long arms are about $Z_{backbone}^{2} \cong 2500$ times larger than the corresponding fluctuations times. For both PI8 and PI11, the consequence is that the constraint release times of the backbone by fluctuations of the long arms are not time-separated from the reptation of the backbone. Moreover, for P11, as shown in figure 12b, reptation of the backbone is slower than fluctuations of the long arms. Therefore, the backbone only relaxes by fluctuations and not by reptation. These results suggest to include the fluctuations solvent of the short arms but to exclude the fluctuations solvent of the long arms to calculate the reptation time of the backbone. The results are shown in Figure 13 and demonstrate an excellent agreement with the experimental results, comparable with that obtained by Frishknecht et al. [23], despite the absence of an adjustable parameter for the “hop length” of the branch point as used by these authors.

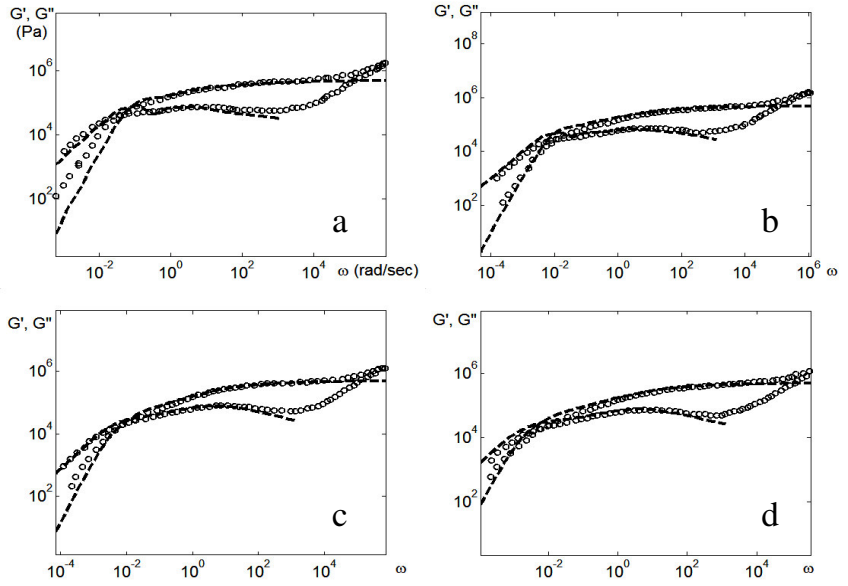

Figure 13: Comparison between predictions (dashed lines) and experimental data (unfilled symbols) of asymmetric star PI8 (a), asymmetric star PI9 (b), asymmetric star PI10 (c) and asymmetric star PI11 (d). The fluctuations solvent of the long arms is not included in the reptation time of the backbone.

4.4.5 Linear Polystyrene (PS) samples with different distributions

To complete the validation of our model, we have tested it on a series of linear PS samples with various molecular weight distributions (monodisperse, bidisperse, polydisperse). We have in particular tested predictions on samples containing a large fraction of poorly entangled chains, since we have previously shown [8] that a sophisticated reptation model including fluctuations (the time-dependent diffusion des Cloizeaux kernel, TDD [46]), while very accurate in many situations, breaks down for systems containing a large fraction of

poorly entangled chains ($M<4.M_e$). We have actually proposed an empirical modification of TDD in order to restore quantitative predictions for those systems. The model presented in the present paper can in principle deal with linear chains since they can be considered as systems of fluctuating and reptating two-arm stars. The inclusion of tube dilation in the reptation and fluctuations processes requires time scale separation as discussed earlier. The critical value of the Graessley number (0.1) allows one to decide about the inclusion or not of the reptation solvent coming from the relaxation of short chains for calculating the relaxation of long ones [4]. In all cases studied here, the solvent fraction to be included in this way has been found to be negligible. For the influence of the reptation solvent on the fluctuations times of the long chains, we have no general criterion. Therefore, we have decided to test both hypotheses and we have found no significant influence.

The material parameters for the model have been fitted on sample PS8 (see Section 3.3) and been used for the predictions on all other samples. The best fit values are 0.23MPa for G_N^0, 16500 g/mol for M_e, and 2.5 10^{-3} s for τ_e. These values compare well with those used in [8]. Figure 14 compares the experimental results and theoretical predictions for a monodisperse sample (PS1) and three well-entangled bidisperse samples (PS8 to PS10), while Figure 15 presents results for bidisperse systems containing a significant fraction of chains with $M<4.M_e$ (PS11 to PS13). In all cases the agreement between experimental and predicted data is excellent, also for systems containing poorly entangled chains, without any adjustment.

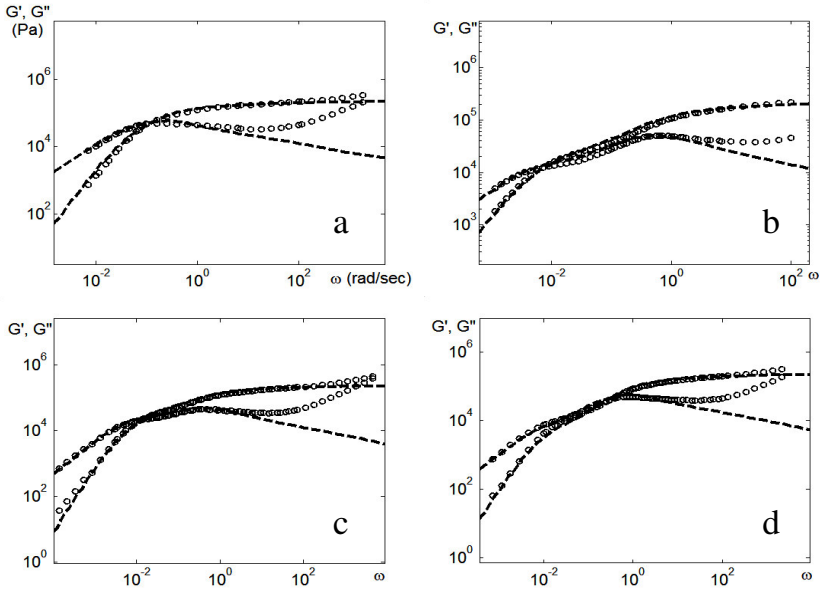

Figure 14: Comparison between predictions (dashed lines) and experimental data (unfilled symbols) of monodisperse linear PS1 (a), bidisperse PS8 (b), bidisperse PS9(c) and bidisperse PS10 (d).

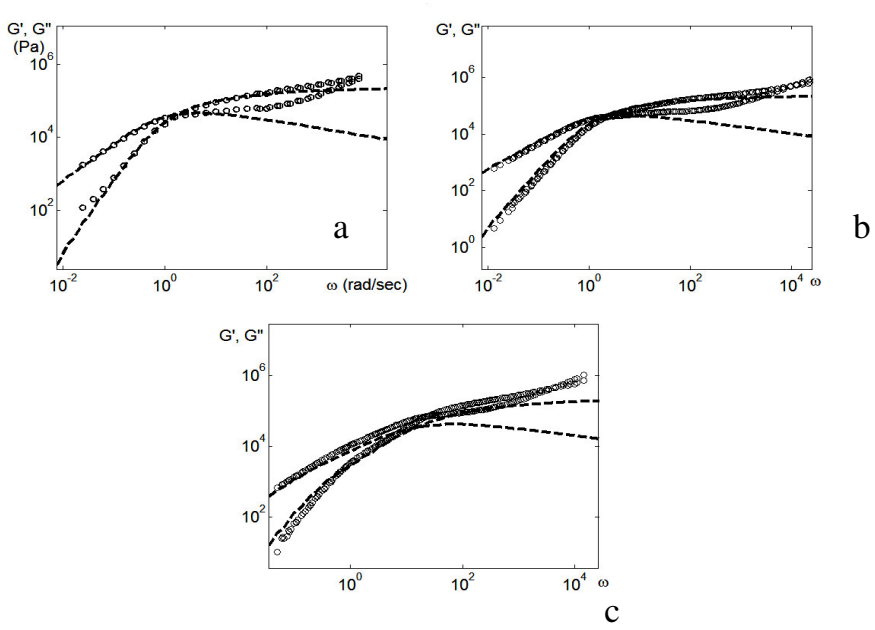

Figure 15: Comparison between predictions (dashed lines) and experimental data (unfilled symbols) for bidisperse PS11 (a),bidisperse PS12 (b) and bidisperse PS13 (c).

4.5 CONCLUSIONS

We have developed and tested a new model suitable for the prediction of linear viscoelasticity from knowledge of molecular structure for arbitrary mixtures of (asymmetric) star and linear entangled molecules. The model is very general and contains the key ingredients of tube models: reptation, fluctuations, constraint release and tube dilation. Reptation and fluctuations in the potential are treated in a classical way. However, we impose no artificial time scale separation between the fluctuations and reptation processes but rather treat both as simultaneous and progressive. Early fluctuations are treated in a new way, simple but effective, based on a potential vs. thermal energy level criterion. This treatment has the advantage to be applicable to

complex mixtures of molecules and gives excellent results. Because the systems modelled can be arbitrary mixtures, there can be no analytical solution and a time-marching algorithm must be used. At each time step, the key parameters to be calculated are the reptation and fluctuations times of each segment. To this end, the interrelations between fluctuations and reptation processes must be taken into account very carefully through the inclusion or exclusion of the constraint release solvent in the considered relaxation process. We have come to the conclusion that a generalization of the concept of "Graessley number" [28], that is the ratio of a characteristic constraint release time over a characteristic relaxation time, can be used as a criterion for the decision to include or exclude the solvent and thus to consider the skinny of the dilated tube for the relaxation process. The model has been tested on a wide range of literature data pertaining to PBD, PI and PS model systems, leading to excellent quality predictions, provided that the constraint release solvent is correctly treated. In particular, we do not need to impose artificial simplifications (reptation as time-step process) or ad hoc parameter modifications for asymmetric stars to get equivalent predictions to those already published. Moreover, with a slight exception concerning the dilution exponent for PI, the same material parameter values can be used for all the corresponding literature data, emphasizing the consistent nature of the proposed model.

REFERENCES

[1] P.G. de Gennes. Reptation of a polymer chain in the presence of fixed obstacles. *J. Chem. Phys.,* 55:572-579, 1971.

[2] M. Doi, S.F. Edwards. *The theory of Polymer Dynamics*. Oxford University Press, 1986.

[3] S.T. Milner, T.C.B. McLeish. Parameter-free theory for stress relaxation in star polymer melts. *Macromolecules*, 30: 2159-2166, 1997.

[4] S.J. Park, R.G. Larson. Tube Dilution and Reptation in Binary Blends of Monodisperse Linear Polymers. *Macromolecules*, 37: 597-604, 2004.

[5] R. Everaers, S.K. Sukumaran, G.S. Grest, C. Svaneborg, A. Sivasubramanian, K. Kremer. Rheology and Microscopic Topology of Entangled Polymeric Liquids. *Science*, 303:823-828, 2004.

[6] F. Léonardi, J-C. Majesté, A. Allal, G. Marin. Rheological models based on the double reptation mixing rule : The effects of a polydisperse environment. *J. Rheol.*, 44:675-692, 2000.

[7] A.E. Likhtman, T.C.B. McLeish. Quantitative theory for linear dynamics of linear entangled polymers. *Macromolecules*, 35:6332-6343, 2002

[8] E. van Ruymbeke, R. Keunings, V. Stéphenne, A. Hagenaars, C. Bailly. Evaluation of reptation models for predicting the linear viscoelastic properties of entangled polymers. *Macromolecules*, 35(7):2689-2699, 2002.

[9] C. Pattamaprom, R.G. Larson, T.J. Van Dyke. Quantitative predictions of linear viscoelastic rheological properties of entangled polymers. *Rheol. Acta*, 39: 517-531, 2000.

[10] F. Léonardi, A. Allal, G. Marin. Determination of the molecular weight distribution of linear polymers by inversion of a blending law on complex viscosities. *Rheol. Acta*, 3:199-213, 1998.

[11] E. van Ruymbeke, R. Keunings, C. Bailly. Determination of the molecular weight distribution of entangled linear polymers

from linear viscoelasticity data. *J. Non-Newtonian Fluid Mech*., 105:153-175, 2002.

[12] R.C. Ball, T.C.B. McLeish. Dynamic dilution and the viscosity of star polymer melts. *Macromolecules*, 29:5717-5722, 1989.

[13] T.C.B. McLeish, S.T. Milner. Entangled dynamics and melt flow of branched polymers. *Adv. Polym. Sci.,* 143:195-256, 1999.

[14] G. Marrucci. Relaxation by reptation and tube enlargement: A model for polydisperse polymers. *J. Polym. Sci., Polym. Phys.*, 23:159-177, 1985.

[15] S.T. Milner. Relating the shear-thinning curve to the molecular weight distribution in linear polymer melts. *J. Rheol.*, 40:303-315, 1996.

[16] C.H. Adams, L.R. Hutchings, P.G. Klein, T.C.B. McLeish, R.W. Richards. Synthesis and Dynamic Rheological Behavior of Polybutadiene Star Polymers. *Macromolecules*, 29:5717-5722, 1996.

[17] T.C.B. McLeish, J. Allgaier, D.K. Bick, G. Bishko, P. Biswas, R. Blackwell, B. Blottière, N. Clarke, B. Gibbs, D.J. Groves, A. Hakiki, R.K. Heenan, J.M. Johnson, R. Kant, D.J. Read, R.N. Young. Dynamics of Entangled H-Polymers: Theory, Rheology, and Neutron-Scattering. *Macromolecules*, 32:6734-6758, 1999.

[18] D.R. Daniels, T.C.B. McLeish, B.J. Crosby, R.N. Young, C.M. Fernyhough. Molecular rheology of comb polymer melts. 1. Linear viscoelastic response. *Macromolecules*, 34:7025-7033, 2001.

[19] T.C.B. McLeish, R.C. Larson. Molecular Constitutive Equations for a Class of Branched Polymers: The Pom-pom Polymer. *J. Rheol.*, 42:82-112, 1998.

[20] B. Blottière, T.C.B. McLeish, A. Hakiki, R.N. Young, S.T. Milner. Rheology and Tube Model Theory of Bimodal Blends of Star Polymer Melts. *Macromolecules*, 31:9295-9304, 1998.

[21] S.T. Milner, T.C.B. McLeish, R.N. Young, A. Hakiki, J.M. Johnson. Dynamic Dilution, Constraint-Release, and Star-Linear Blends. *Macromolecules*, 31:9345-9353, 1998

[22] J.H. Lee, L.A. Archer. "Stress relaxation of star/linear polymer blends. *Macromolecules*, 35:6687-6696, 2002

[23] A.L. Frischnecht, S.T. Milner, A. Pryke, R.N. Young, R. Hawkins, T.C.B. McLeish. Rheology of Three-Arm Asymmetric Star Polymer Melts. *Macromolecules*, 35:4801-4820, 2002

[24] D.J. Read, T.C.B. McLeish. Molecular Rheology and Statistics of Long Chain Branched Metallocene-Catalyzed Polyolefins. *Macromolecules*, 34:1928-1945, 2001.

[25] R.G. Larson. Combinatorial Rheology of Branched Polymer Melts. *Macromolecules*, 34: 4556-4571, 2001.

[26] R.J. Blackwell, O.G. Harlen, T.C.B. McLeish. Theoretical Linear and Nonlinear Rheoloy of Symmetric Treelike Polymer Melts. *Macromolecules*, 34:2579-2596, 2001.

[27] N.J. Inkson, T.C.B. McLeish. Predicting low density polyethylene melt rheology in elongational and shear flows with "pom-pom" constitutive equations, *J. Rheol*., 43:873-896, 1999.

[28] M.J. Struglinski, W.W. Graessley. Effects of Polydispersity on the Linear Viscoelastic Properties of Entangled Polymers. 1. Experimental Observations for Binary Mixtures of Linear Polybutadienes. *Macromolecules*, 18:2630-2643, 1985

[29] S.J. Park, R.G. Larson. Dilution exponent in the dynamic dilution theory for polymer melts. *J. Rheol.,* 47:199-211, 2003.

[30] R.H. Colby, M. Rubinstein. Two-parameter scaling for polymers in θ solvents. *Macromolecules*, 23:2753-2757, 1990.

[31] V.R. Raju, E.V. Menezes, G. Marin, W.W. Graessley. Concentration and molecular weight dependence of viscoelastic properties in linear and star polymers. *Macromolecules*, 14:1668-1676, 1981.

[32] C. Tsenoglou. Viscoelasticity of binary polymer blends, *ACS Poym. Preprints* 28: 185-186, 1987

[33] J. des Cloizeaux. Double reptation *vs* simple reptation in polymer melts. *J. Europhys. Lett*., 5 :437-442, 1988

[34] J.L. Viovy, M. Rubinstein, R.H. Colby.Constraint release in polymer melts: tube reorganization versus tube dilution. *Macromolecules*, 24: 3587-3596, 1991

[35] R.G. Larson, T. Sridhar, L.G. Leal, G.H. McKinley, A.E. Likhtman, T.C.B. McLeish. Definitions of entanglement spacing and time constants in the tube model. *J. Rheol.* 47:809-818, 2003.

[36] P.F. Green, P.J. Mills, C.J. Palmstrom, J.W. Mayer, E.J. Kramer. The limits of reptation in polymer melts. *Phys. Rev. Lett.*, 53:2145-2148, 1984.

[37] P.F. Green, E.J. Kramer. Matrix Effects on the Diffusion of Long Polymer Chains. *Macromolecules*, 19:1108-1114, 1986.

[38] F.R. Schwarzl, Numerical calculation of storage and loss modulus from stress relaxation data for linear viscoelastic materials, *Rheol. Acta*, 10:166-173, 1971

[39] J. Roovers. Tube renewal in the relaxation of 4-arm star polybutadienes in linear polybutadienes. *Macromolecules*, 20:148-152, 1987.

[40] M. Baumgaertel, M.E. de Rosa, J. Machado, M. Masse, H.H. Winter. The relaxation time spectrum of nearly monodisperse polybutadiene melts. *Rheol. Acta*, 31:75-82, 1992.

[41] M.J. Struglinski, W.W. Graessley. Effects of Polydispersity on the Linear Viscoelastic Properties of Entangled Polymers. 3. Experimental Observations on Binary Mixtures of Linear and Star Polybutadienes. *Macromolecules*, 21:783-789, 1988.

[42] Data kindly provided by C. Friedrich and D. Schulze, from FMF (Freiburg, Germany).

[43] L.J. Fetters, D.J. Lohse, D. Richter, T.A. Witten, A. Zirkel. Connection between polymer molecular weight, density, chain dimensions, and melt viscoelastic properties. *Macromolecules*, 27: 4639-4647, 1994.

[44] J.D. Ferry. *Viscoelasic properties of polymers*. Wiley, New York, 1980

[45] *Experimental relaxation moduli of PI2 multiplied by a factor (411/230), like in [20].*

[46] J. des Cloizeaux. Relaxation and Viscosity Anomaly of Melts Made of Long Entangled Polymers. Time-Dependent Reptation. *Macromolecules*, 23:4678-4687, 1990.